Residual Resistivity of Concentrated Ferromagnetic Disordered Alloys*

F. Brouers†
Laboratoire de Physique des Solides,‡ Faculté des Sciences, 91 Orsay, France
and
A. V. Vedyayev
University of Moscow, Faculty of Sciences, Moscow, U.S.S.R.
and
M. Giorgino
Institut de Physique, Université de Liège, Liège, Belgium
(Received 9 March 1972)

A theory of the residual electrical resistance of ferromagnetic disordered alloys is presented in the framework of the coherent-potential approximation. It generalizes a previous calculation made for a two-band model Hamiltonian relevant for transition-metal-based alloys. This formalism can be applied to calculate the concentration dependence of magnetization, spin-up and spin-down resistivities, and spontaneous resistivity anisotropy of ferromagnetic alloys. These quantities are computed for a simple model of NiCu and are found to be in good agreement with observation.

I. INTRODUCTION

In a series of papers[1-5] a two-s-d-band model Hamiltonian has been applied to discuss qualitatively the concentration dependence of some typical electronic and transport properties of concentrated transition- and noble-metal alloys.

This model Hamiltonian was first introduced by Levin and Ehrenreich[1] (hereafter referred to as LE). The purpose of LE's paper was twofold: first, to discuss the general properties of this model in the framework of the coherent-potential approximation (CPA) introduced by Soven[6,7] and Velicky *et al.*,[8] and second, to use it as a simplified Hamiltonian relevant to investigate the concentration dependence of the charge transfer and the optical-absorption edge of AgAu.

The LE model has been extended[2,3] to take account of both s-d hybridization and d hopping (LEBV model). With that model Hamiltonian two of us have shown[3] that it is possible to write down within the CPA expressions for the residual resistivity which explain the deviations from Nordheim's rule observed in some transition-metal-based alloys.

Finally, in a paper[4] reviewing the previous contributions, a self-consistent calculation of the charge transfer which improves the results obtained in Ref. 1 was presented and the LEBV model was extended in order to investigate the magnetic properties of concentrated disordered ferromagnetic transition-metal alloys.

It is the purpose of the present paper to show that this generalized formalism is also able to describe semiquantitatively the concentration dependence of typical magnetic properties, such as the spontaneous resistivity anisotropy in nondilute ferromagnetic alloys. This effect measures the difference between the resistivities of currents parallel and perpendicular to the magnetization in ferromagnetic metals and alloys. There is strong evidence that the spin-orbit coupling is responsible for this effect. Smit[9] proposed a simple theory along these lines. The spin-orbit coupling produces a mixing of spin-up and spin-down states which is not isotropic because the magnetization provides an axis for the spin-orbit coupling. As shown by Campbell, Fert, and Jaoul[10,11] for small concentrations, the two-current picture of Mott[12] substantiates this theory by convincingly relating the spin-up and spin-down resistivity to the spontaneous anisotropy of the resistivity in some Ni-based alloys for which data are available. For nondilute alloys, it was interesting to test the LEBV model and to see to what extent the CPA theory of the dc conductivity discussed in Refs. 13 and 3 is able to account for the concentration dependence of the resistance anisotropy observed in Ni-based alloys.[14]

We shall now give an outline of the paper. In Sec. II the LEBV model for paramagnetic alloys is characterized in the CPA. In Sec. III this model is generalized to ferromagnetic alloys and expressions for the majority- and minority-spin density of states are derived. The d disorder is treated within the CPA, while the exchange interaction is treated in the Hartree-Fock approximation.

In Secs. IV and V a numerical calculation of the concentration dependence of the magnetic properties of a model of concentrated NiCu alloy is presented. The magnetization, ratio of spin-down

and spin-up resistivities, total resistivity, and, finally, spontaneous anisotropy of the resistivity are found to be in good agreement with experimental data.

II. MODEL

In the LEBV model the pure metals A and B forming the substitutional disordered A_xB_{1-x} alloys are assumed to have a broad s band and a narrow d band centered at energy $\epsilon_d^{A(B)}$. The effect of the degeneracy is neglected. In the A_xB_{1-x} alloy, the d energy level at a given site may be ϵ_d^A or ϵ_d^B, corresponding to whether the site n is occupied by an A or a B atom, respectively, with probability x and $1-x$. The unhybridized s bands and the hybridization parameters are assumed to exhibit the virtual-crystal behavior. By contrast, the disorder associated with the d band is treated in the framework of the multiple scattering theory.

For a given configuration of the alloy, the Hamiltonian reads

$$H=\sum_{k\in \mathrm{BZ}} E_s(k)|k_s\rangle\langle k_s| + \sum_{k\in \mathrm{BZ}} \epsilon_d(k)|k_d\rangle\langle k_d| + \sum_n \epsilon_d^{A(B)}|n_d\rangle\langle n_d| + \sum_{k\in \mathrm{BZ}} \gamma_H(|k_s\rangle\langle k_d| + |k_d\rangle\langle k_s|) . \quad (1)$$

The first two terms correspond to the kinetic energy of the s and d electrons. The third term where the state $|n_d\rangle$ represents the Wannier states on site n,

$$|n_d\rangle = N^{-1}\sum_{k_d} e^{-ik_d R_n}|k_d\rangle , \quad (2)$$

contains the random d levels. The last term, where the coupling constant γ_H is assumed to be k independent, accounts for the s-d hybridization. The value of the $E_s(k)$ dispersion relation at the Brillouin-zone (BZ) boundaries determines the width $2W_s$ of the unhybridized s band:

$$E_s(k) = E_0^{A(B)} + \epsilon_s(k)$$

with

$$\epsilon_s(k) = W_s s(k), \quad -1 \leq s(k) \leq 1 . \quad (3)$$

As indicated before, the s-band and hybridization parameters in the alloy satisfy

$$E_0 \to \bar{E} = xE_0^A + (1-x)E_0^B ,$$

$$\gamma_H \to \bar{\gamma}_H = x\gamma(\epsilon_d^A) + (1-x)\gamma(\epsilon_d^B) .$$

We assume that the unhybridized s and d bands have the same shape but differ in location and width. We also assume, for convenience, a semielliptic shape. If the energy origin is chosen midway between the constituent d levels, we have

$$\bar{E}_s(k) = \bar{E} + \epsilon_s(k), \quad \epsilon_d(k) = \alpha\epsilon_s(k) . \quad (4)$$

The parameter α specifies the relative width of the s and d bands.

In the paramagnetic case[1,3] it was shown that in the CPA the s and d density of states is obtained from

$$n_s(E) = -\nu_s \frac{1}{\pi}\mathrm{Im}F_{ss}(E+i0) ,$$
$$n_d(E) = -\nu_d \frac{1}{\pi}\mathrm{Im}F_{dd}(E+i0) , \quad (5)$$

where ν_s and ν_d are the total number of states available in the bands and $F_{ss}(z)$ and $F_{dd}(z)$ are, respectively,

$$F_{ss}(z) = N^{-1}\sum_k \langle k_s|\bar{G}(z)|k_s\rangle$$

and (6)

$$F_{dd}(z) = N^{-1}\sum_k \langle k_d|\bar{G}(z)|k_d\rangle ,$$

and are determined from the averaged Green's function:

$$\bar{G}(z) = \begin{pmatrix} z - E_s(k) & -\bar{\gamma}_H \\ -\bar{\gamma}_H & z - \epsilon_d(k) - \Sigma_d(z) \end{pmatrix}^{-1} \quad (7)$$

where the overbar indicates a configuration average. The self-energy $\Sigma_d(z)$ is defined by the self-consistent relation (see Ref. 3)

$$\Sigma_d^{\mathrm{CPA}}(z) = \bar{\epsilon} + \frac{x(1-x)(\epsilon_d^A - \epsilon_d^B)^2 F_{dd}(z,\ \Sigma_d)}{1 + (\bar{\epsilon} + \Sigma_d)F_{dd}(z,\ \Sigma_d)} , \quad (8)$$

where $\bar{\epsilon}$ is the average energy $\bar{\epsilon} = x\epsilon_d^A + (1-x)\epsilon_d^B$. A simple expression for $F_{dd}(z,\ \Sigma_d)$ can be derived from (6) and (7) if we know the s density of states of the pure metals $\rho_{0s}(E)$:

$$F_{dd}(z,\ \Sigma_d) = \int d\epsilon \frac{\rho_{0s}(E)}{z - \Sigma_d(z) - \alpha E - \bar{\gamma}_H^2(z - E - \bar{E})^{-1}}$$

and can easily be expressed (cf. Refs. 1–3) in terms of $F_{0s}(E)$, the Hilbert transform of $\rho_{0s}(E)$. This formalism can be generalized to ferromagnetic alloys. We shall examine this extension of the theory in Sec. III.

III. GENERALIZATION OF CPA TO FERROMAGNETIC ALLOYS

As for the one-band model,[15] this formalism can be generalized to calculate the magnetic properties of transition-metal-based alloys.[4] As a first step, as in Ref. 15, we adopt in this paper the Hartree–Fock approximation. The most important contribution comes from the Coulomb repulsion between two antiparallel d electrons on the same orbital:

$$H_{\mathrm{cor},\mu} = U_\mu^{d-d}\sum_i N_{d,\mu,\sigma}^i N_{d,\mu,-\sigma}^i , \quad (9)$$

with

$$U_{\mu}^{d-d}=\int \Phi_{\mu}^{*}(\vec{r}_1)\,\Phi_{\mu}^{*}(\vec{r}_2)e^2|r_1-r_2|^{-1}\Phi_{\mu}(\vec{r}_2)\Phi_{\mu}(\vec{r}_1)\,d^3\vec{r}_1\,d^3\vec{r}_2\,, \tag{10}$$

where the indices i, μ, σ denote the site, the orbital, and the spin, respectively, and $N_{d,\mu,\sigma}^{i}$ is the average number of electrons in that state. In this paper we shall neglect the effect of the degeneracy and consider the d band as a whole. Since the model Hamiltonian (1) refers to the paramagnetic alloy, we shall describe the ferromagnetic alloy by adding to (1) the following term:

$$H_{\rm cor}^{\rm ferro}-H_{\rm cor}^{\rm para}\,. \tag{11}$$

In the Hartree–Fock approximation, the ferromagnetic model Hamiltonian will have the same form as (1) but with a spin dependence of the d-resonance levels:

$$\epsilon_{d,\sigma}^{A(B)}=\epsilon_{\rm para}^{A(B)}-U_{\rm eff}^{A(B)}\,(N_{d,-\sigma}^{A(B)}-N_{d,-\sigma}^{A(B)\rm para})\,. \tag{12}$$

The energy $U_{\rm eff}^{A(B)}$ is an effective d-d exchange energy whose value will depend on the number of d electrons considered in the model as well as contributions other than (9). The number of electrons per atom $N_{d,\pm\sigma}^{A(B)}$ does not depend on the site but depends on the atom occupying the site. The CPA is easily generalized. The self-energy is now spin dependent:

$$\Sigma_d^{\sigma}(z)=\bar{\epsilon}_{d,\sigma}-(\epsilon_{d,\sigma}^{A(B)}-\Sigma_d^{\sigma})F_{dd}^{\sigma}(z,\Sigma_d^{\sigma}(z))(\epsilon_{d,\sigma}^{A(B)}-\Sigma_d^{\sigma})\,, \tag{13}$$

with

$$\bar{\epsilon}_{d,\sigma}=x\,\epsilon_{d,\sigma}^{A}+(1-x)\epsilon_{d,\sigma}^{B}\,. \tag{14}$$

The s and d densities of states are now given by

$$n_{s,\sigma}(E)=\frac{\nu_s}{2\pi}\,{\rm Im}F_{ss}^{\sigma}(z,\Sigma_d^{\sigma}(z))\,|_{z=E+i0} \tag{15}$$

and

$$n_{d,\sigma}(E)=-\frac{\nu_d}{2\pi}\,{\rm Im}F_{dd}^{\sigma}(z,\Sigma_d^{\sigma}(z))\,|_{z=E+i0}\,, \tag{16}$$

while the partial d density of states on atoms A and B are straightforward generalizations of the expressions derived in the one-band model (Ref. 8) when one averages over random configurations with an atom of type A or B located at site $n=0$:

$$\begin{aligned} n_{d,\sigma}^{A(B)}&=-\frac{\nu_d}{2\pi}\,{\rm Im}\langle\, n_d=0\,|\,\{z-H_{\rm eff}^{\sigma}(z)-|\,0\rangle(\epsilon_{d,\sigma}^{A(B)}-\Sigma_d^{\sigma})\langle 0\,|\}^{-1}\,|\,n_d=0\rangle\,|_{z=E+i0}\\ &=-\frac{\nu_d}{2\pi}\,{\rm Im}\,\frac{F_{dd}^{\sigma}(z,\Sigma_d^{\sigma}(z))}{1-[\epsilon_{d,\sigma}^{A(B)}-\Sigma_d^{\sigma}(z)]F_{dd}^{\sigma}(z,\Sigma_d^{\sigma}(z))}\,\Bigg|_{z=E+i0}\,. \end{aligned} \tag{17}$$

Here $H_{\rm eff}$ is the single-site CPA effective Hamiltonian defined by $\bar{G}=(z-H_{\rm eff})^{-1}$ and corresponding to a d self-energy Σ_d on every atomic site.

In the Appendix, we show how a $\bar{t}$ approximation can be used in the ferromagnetic case as the starting point of the iteration procedure leading to the self-consistent solution of Eq. (13).

Since $\epsilon_{d,\sigma}^{A(B)}$ is a function of the number of d electrons $N_{d,-\sigma}^{A(B)}$, the ferromagnetic solution is obtained by solving the five simultaneous equations with five unknowns, the Fermi energy E_F, and $N_{d,\pm\sigma}^{A(B)}$:

$$N_{d,\pm\sigma}^{A(B)}=\int_{-\infty}^{E_F}n_{d,\pm\sigma}^{A(B)}(E)\,dE=N(N_{d,\mp\sigma}^{A},N_{d,\mp\sigma}^{B}) \tag{18}$$

and

$$xN_0^A+(1-x)\,N_0^B=\int_{-\infty}^{E_F}dE[n_{s,\sigma}(E)+n_{s,-\sigma}(E)+n_{d,\sigma}(E)+n_{d,-\sigma}(E)]\,, \tag{19}$$

where $N_0^{A(B)}$ represents the total number of s and d electrons of pure $A(B)$ metal. When these five equations are solved, the average magnetic moment per atom of the alloy is equal to

$$\bar{\mu}=x\,\mu^{A}+(1-x)\,\mu^{B}\,, \tag{20}$$

with

$$\mu^{A(B)}=(N_{d,\sigma}^{A(B)}-N_{d,-\sigma}^{A(B)})\mu_B\,, \tag{21}$$

where μ_B is the Bohr magneton. As we shall see in the discussion of Sec. IV, this formulation can account for the splitting of spin-up and spin-down bands in pure metals as well as the concentration dependence of this splitting in disordered alloys.

IV. SPIN-DEPENDENT RESISTIVITY

In the same way, the formalism we have derived in Ref. 3 to calculate the dc electrical conductivity in the LEBV model can be generalized to deal with ferromagnetic alloys. We have shown that provided the following approximations are made in the model: (i) The random potentials are short ranged; (ii) the coupling constant γ_H is k independent; (iii) the matrix elements $\langle n_s\,|\,\hat{R}\,|\,n_d\rangle$ of $\hat{R}$ (the site-position operator between s and d Wannier states) are identically zero, the CPA vertex corrections in the expression of the dc conductivity vanish, and the conductivity can be written as a sum of three contributions:

$$\sigma=\sigma_{ss}+2\sigma_{sd}+\sigma_{dd} \tag{22}$$

represented by the diagrams of Fig. 1. In ferromagnetic alloys the self-energy due to d scattering is spin dependent and, since the spin-up and spin-down bands are split, the two quantities $\Sigma_d^{\sigma}(E_F)$ and $\Sigma_d^{-\sigma}(E_F)$ are different at the Fermi energy. There-

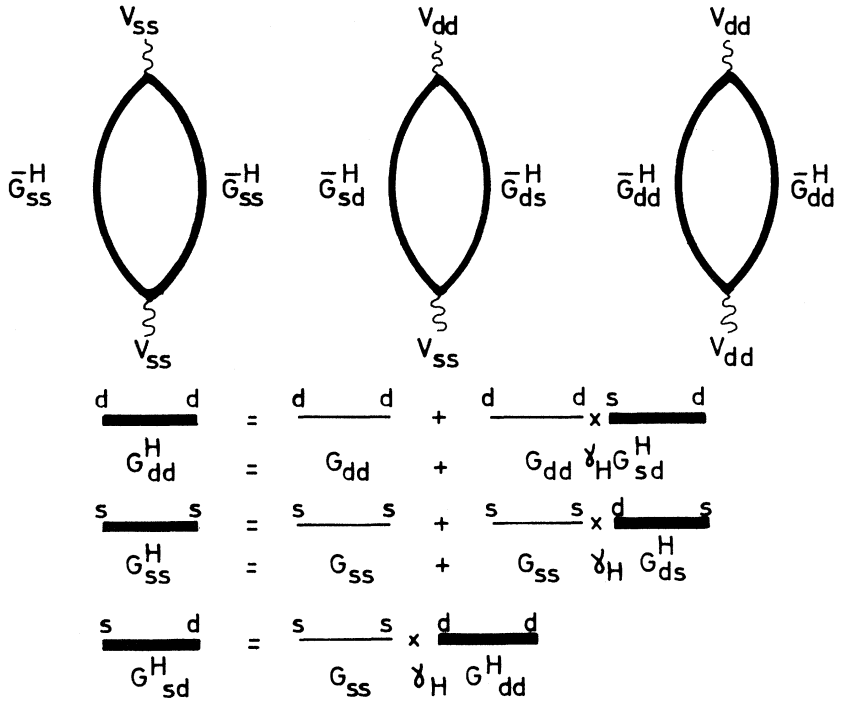

FIG. 1. Diagrammatic representation of the various contributions to the dc electrical conductivity.

fore, at low temperature, where magnon interaction giving rise to spin-flip mechanism is negligible, the total conductivity can be viewed as the sum of the conductivities of two currents:

$$\sigma = \sigma^{\uparrow} + \sigma^{\downarrow} . \tag{23}$$

The contributions $\sigma^{\uparrow(\downarrow)}_{ss}$, $\sigma^{\uparrow(\downarrow)}_{sd}$, and $\sigma^{\uparrow(\downarrow)}_{dd}$ are simple generalizations of Eq. (57) of Ref. 3:

$$\sigma^{\uparrow(\downarrow)}_{ss} = \nu_s \frac{e^2}{\pi\Omega_c}\int d\eta \left(-\frac{df}{d\eta}\right)\sum_k v_s^2(k) \times [\mathrm{Im}\bar{G}_{ss}(k, \Sigma^{\uparrow(\downarrow)}_d, \eta + i0)]^2 , \tag{24a}$$

$$\sigma^{\uparrow(\downarrow)}_{dd} = \nu_d \frac{e^2}{\pi\Omega_c}\int d\eta \left(-\frac{df}{d\eta}\right)\sum_k v_d^2(k) \times [\mathrm{Im}\,\bar{G}_{dd}(k, \Sigma^{\uparrow(\downarrow)}_d, \eta + i0)]^2 , \tag{24b}$$

$$\sigma^{\uparrow(\downarrow)}_{sd} = \sigma^{\uparrow(\downarrow)}_{ds} = (\nu_s \nu_d)^{1/2} \frac{e^2}{\pi\Omega_c}\int d\eta \left(-\frac{df}{d\eta}\right)\sum_k v_s(k) v_d(k) \times [\mathrm{Im}\,\bar{G}_{sd}(k, \Sigma^{\uparrow(\downarrow)}_d, \eta + i0)]^2 , \tag{24c}$$

where Ω_c is the volume of the unit cell and $f(\eta)$ is the Fermi–Dirac distribution function. Provided we choose, as in Ref. 3, a simple expression for the velocity function $\phi(E)$,

$$\phi(E) = N^{-1}\sum_k v_s^2(k)\,\delta(E - E_s(k)) \propto (W_s^2 - E^2)^{3/2} , \tag{25}$$

we can use Eqs. (24a)–(24c) to compute the concentration dependence of the minority- and majority-spin-band residual resistivities of alloys in the ferromagnetic state at $T = 0$,

$$\rho^{\downarrow} = 1/\sigma^{\downarrow}, \quad \rho^{\uparrow} = 1/\sigma^{\uparrow}, \tag{26}$$

as well as the concentration dependence of the total resistivity,

$$\rho = \frac{\rho^{\uparrow}\rho^{\downarrow}}{\rho^{\uparrow} + \rho^{\downarrow}} . \tag{27}$$

V. SPONTANEOUS ANISOTROPY OF RESISTANCE

At low temperature the ratio of minority- and majority-band resistivities is a characteristic quantity for a given alloy. Campbell, Fert and Jaoul[10,11] have used the two-current model to evaluate this quantity for various Ni-based alloys. They suppose that transport at low temperature, in the absence of spin-orbit coupling but in the presence of impurities, is by two parallel currents of electrons, spin ↑ and spin ↓, each with its own residual resistivity $\rho^{\uparrow}$ and $\rho^{\downarrow}$, and they show that, for temperatures well below the Curie temperature and for concentrations such that the impurities do not interact, this ratio is fixed for a given impurity and is independent of concentration. The numerical application of the CPA formalism which we present in Sec. VI indicates that this statement is true in that case, for concentrations lower than (6–7)%. In the presence of spin-orbit coupling there is a mixing of spin-up and spin-down states which is

not isotropic and gives rise to an anisotropy of the resistance. Experimentally, the spontaneous anisotropy of the resistance is defined by

$$\frac{\Delta\rho}{\rho_{av}} = 2\left(\frac{\rho_{\parallel}-\rho_{\perp}}{\rho_{\parallel}+\rho_{\perp}}\right) , \tag{28}$$

where $\rho_{\parallel}$ and $\rho_{\perp}$ are measured parallel and perpendicular to the magnetization at saturation and extrapolated to $B=0$. Smit's theory gives a simple expression relating $\Delta\rho/\rho_{av}$ to $\rho\downarrow/\rho\uparrow$.

Assuming a tight-binding model for the d states and an exchange field $\mathcal{H}_{ex}$ but no crystal field, Smit has shown using a simple perturbation calculation that the effect of mixing spin-up and spin-down states (and hence the resistivity change) is stronger for an electron traveling along the magnetization direction than for one traveling perpendicular to it. At low temperature when the spin-mixing term due to magnons is negligible, one has[16]

$$\begin{aligned}\rho_{\uparrow}^{\parallel} &= \rho_{\uparrow}^{\perp} + \gamma_{so}\rho\downarrow ,\\ \rho_{\downarrow}^{\parallel} &= \rho_{\downarrow}^{\perp} - \gamma_{so}\rho\downarrow ,\end{aligned} \tag{29}$$

where $\rho\downarrow$ is the resistance for spin-down electrons in the absence of spin-orbit coupling and γ_{so} is a constant depending on the spin-orbit coefficient A and the internal exchange field:

$$\gamma_{so} = \frac{3}{4}\left(\frac{A}{\mathcal{H}_{ex}}\right)^2 . \tag{30}$$

When these changes are put into the expression for the total resistivity, one finds at low temperature

$$\frac{\rho_{\parallel}-\rho_{\perp}}{\rho_{av}} = \gamma_{so}\left(\frac{\rho\downarrow}{\rho\uparrow} - 1\right) . \tag{31}$$

In the dilute limit γ_{so} is a quantity characteristic of the host. For instance, the value which best fits the experimental results is, for Ni-based alloys,[10,11]

$$\gamma_{so} \simeq 0.0075 .$$

For small concentrations $\rho\downarrow/\rho\uparrow$ is independent of cencentration and one would expect the same property for $\Delta\rho/\rho_{av}$ if γ_{so} is assumed to be constant.

Roughly, such behavior is observed indeed in *Ni*Co, *Ni*Fe, *Ni*Mn, *Ni*V, and *Ni*Cr at low concentrations ($\lesssim 5$ at.%). For higher concentrations, the quantities γ_{so} and $\rho\downarrow/\rho\uparrow$ will vary with concentration, and the exact concentration dependence of $\Delta\rho/\rho_{av}$ is less easily predicted. In all Ni-based alloys[14] the anisotropy tends to decrease with concentration and the exact concentration dependence of $\Delta\rho/\rho_{av}$ is less easily predicted. In some of them, however, there is first an increase of the anisotropy (in *Ni*Co, for example) or a large range of concentration where this quantity is constant (in *Ni*Fe). To understand this varying behavior, it is necessary to know the concentration dependence of both factors γ_{so} and $\rho\downarrow/\rho\uparrow$. The theory developed in Secs. II and III provides a method to give such information and hence to extend the theory of the spontaneous resistivity anisotropy to nondilute alloys. In Sec. VI we report the result of a numerical calculation made for a LEBV-model alloy relevant to discuss the magnetic properties of NiCu.

VI. NUMERICAL ILLUSTRATIONS

In this section a physical picture of the ferromagnetic NiCu alloy system is developed which reproduces some of its salient qualitative features. In particular, we shall examine the concentration dependence of the Bohr-magneton number, the total resistivity, the ratio of the minority- and majority-band resistivities $\rho\downarrow/\rho\uparrow$, and finally the spontaneous resistivity anisotropy. The choice of approximation and parameters for the pure systems will be now justified and summarized.

A. Pure Metals

In the two-band model characterized in Secs. II and III, one usually takes a simple shape for the s and d unhybridized bands of pure metals to avoid cumbersome analytical and numerical calculations. We shall do the same here. A semielliptic band is not, however, able to reproduce correctly the behavior of Cu and Ni densities of states at the top of the band. In ferromagnetic metals and alloys, the position of the Fermi level and the density of states at the Fermi level are of primary importance when one is interested in finding the ferromagnetic solution and calculating the transport properties. For that reason, we shall make a further approximation. We shall consider only electrons of the upper peak of the d density of states appearing in band-structure calculations for Ni and Cu (for instance, Hodges *et al.*[17]) and describe them with a LEBV model. The presence of the lower part of the d density of states will be ignored in our calculation. This is justified as far as we suppose that, in ferromagnetic metals like Ni, the net spin density is determined largely by electrons near the top of the d band, rather than by electrons throughout the entire band structure which must be considered rather in connection with the total charge density. To characterize the pure systems, we have to give numbers to the following quantities: ν_s and ν_d, the total number of s and d states in the band; the position of the d potential $\epsilon_{para}^{A(B)}$; the hybridization constants $\gamma_H^{A(B)}$; the exchange effective interaction energy U_{eff}; the width of the s band W_s which will be taken as the energy unit; and the factor α giving the ratio of the s and d unhybridized bandwidths.

We did not try to find the optimum set of parameters but rather used reasonable values which

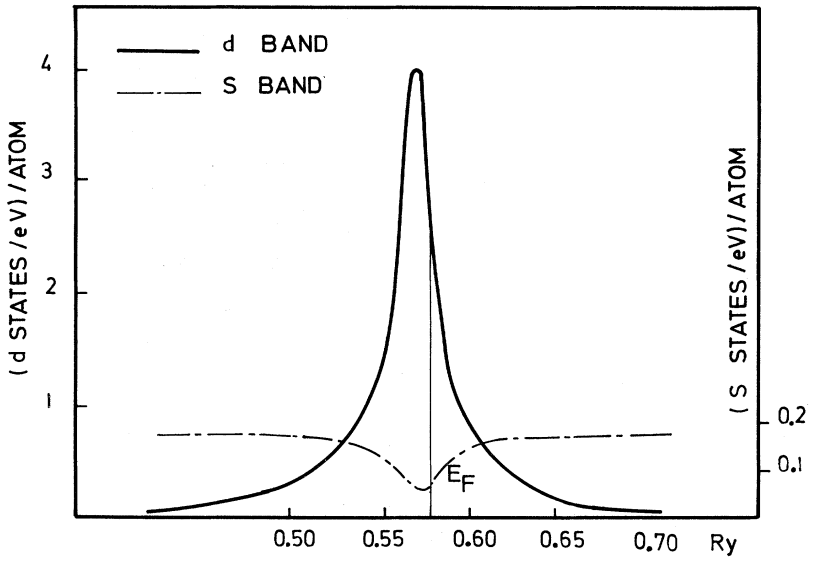

FIG. 2. s band and the upper peak of the a band used to represent paramagnetic Ni.

give numerical results which are within the range of theoretical and experimental estimations for the density of states of Cu and Ni and the magnetic properties of Ni.

According to the previous discussion, we consider only d electrons in the peak at the top of the d band, the volume of which is, for both Cu and Ni, roughly 3 electrons per atom. Therefore, we take $\nu_d = 3$ for the d band and $\nu_s = 2$ for the s band. The position of the peak in the band-structure calculation of Ref. 16 provides us with the values $\epsilon^{Ni}_{para} = 7.75$ eV and $\epsilon^{Cu}_{para} = 5.50$ eV. The k-independent hybridization constant for the two metals is $\gamma_H = 1$ eV, in accordance with Heine's discussion of hybridization in transition metals.[18] To reproduce the upper peak obtained in the band-structure calculation of paramagnetic Cu and Ni, we have taken, moreover, the following values for α and W_s: $\alpha = 0.0275$, which is large enough to eliminate any structure reminiscent of the hybridization gap appearing for $\alpha = 0$; and $W_s = 7.2$ eV, which is quite reasonable for transition and noble metals. The unhybridized s bands are the same for Cu and Ni. As we neglect the contribution of seven electrons of the lower part of the d band, we consider a population of three electrons for Ni and four electrons for Cu.

Figure 2 reproduces the upper part of the paramagnetic Ni density of states calculated with these parameters. We get the correct value for the maximum of the density of states (~ 2 states per eV per atom). Because of the sharp variation of the density of states in that region, the density of states at the Fermi energy $n(E_F)$ is slightly smaller than that calculated in Ref. 17. The number of d holes in Ni is found to be 1.10. This is larger than the 0.6 usually assumed but in accordance with the conclusions of Hodges *et al.*[17] We get the same kind of agreement for Cu.

To determine the ferromagnetic solution for Ni, an estimate of U^{Ni}_{eff} is needed. We have taken for the effective correlation interaction a value such that $n_\sigma(E_F)U_{eff} = 1.2$, which is the value generally attributed to Ni in connection with the Stoner criterion of ferromagnetism[19]: $n_\sigma(E_F)U_{eff} > 1$, where the quantity $n_\sigma(E_F)$ is the density of states at the Fermi energy for one spin. In our model this gives $U_{eff} = 0.9$ eV, a reasonable value[20] which gives a splitting of $U_{eff}(N\uparrow - N\downarrow) = U_{eff}(1.25 - 0.65) = 0.54$ eV and a magnetic moment of $0.6\mu_B$ per atom.

Figure 3 shows the upper part of the Ni d density of states in the ferromagnetic phase calculated in our model. The position of the Fermi level with respect to the splitting of the d band is in agreement with band-structure calculations. An interesting feature of this model is that hybridization gives rise to a depletion of the s density of states where the d density of states is maximum. Because of the band splitting, at Fermi energy this effect is more pronounced in the minority s band than in the majority s band. As a consequence $n^{\uparrow}_s(E_F) > n^{\downarrow}_s(E_F)$, in contrast with the total density of states $n\uparrow(E_F) < n\downarrow(E_F)$. This could be a possible partial explanation of the polarization effect observed in spin-dependent tunneling experiments[21] when the density of states of the majority band appears to be larger than that of the minority band, if one assumes that in such experiments of the role of s electrons is more important than that of d electrons. Here the difference between $n^{\uparrow}_s(E_F)$ and $n^{\downarrow}_s(E_F)$ is about 50% compared to about 10% reported in Ref. 21 and by Bänninger *et al.* in photoemission experiments.[22] This dif-

ference could be due either to the crudeness or overestimation of hybridization in our model or to the influence of the d-electron contribution to the tunneling. As these features are concentration dependent in alloys, it would be interesting to investigate this effect in Ni-based alloys.

B. Alloy

Figures 4–11 illustrate the application of the formalism developed in Secs. II–V to alloys of the two artificial metals corresponding to Cu and ferromagnetic Ni which we have characterized in Sec. VI A. Since only one metal is ferromagnetic, the calculation of the ferromagnetic solution can be done with precision up to 40 at.% Cu in Ni. The computed number of Bohr magnetons decreases linearly (see Fig. 6) and agrees with experimental data.[23] For a concentration of Cu higher than 40 at.%, the solution is less accurate, experimental data are scarce, and the alloy can no longer be considered as completely disordered. For that reason, the results have been extrapolated for higher concentrations (broken line). Figures 4 and 5 represent the density of states for two concentrations, 6 and 30 at.% Cu. It is found that the Fermi level does not move as the concentration of Cu increases, while the band splitting decreases almost linearly with concentration. Figure 7 shows the variation of the low-T specific-heat coefficient γ vs concentration measured by Dixon *et al.*[23] The dashed line represents the variation with concentration of the density of states at the Fermi energy, which is seen to be in reasonably good agreement. The small feature at very small concentration may be due to an overestimation of the effect of hybridiza-

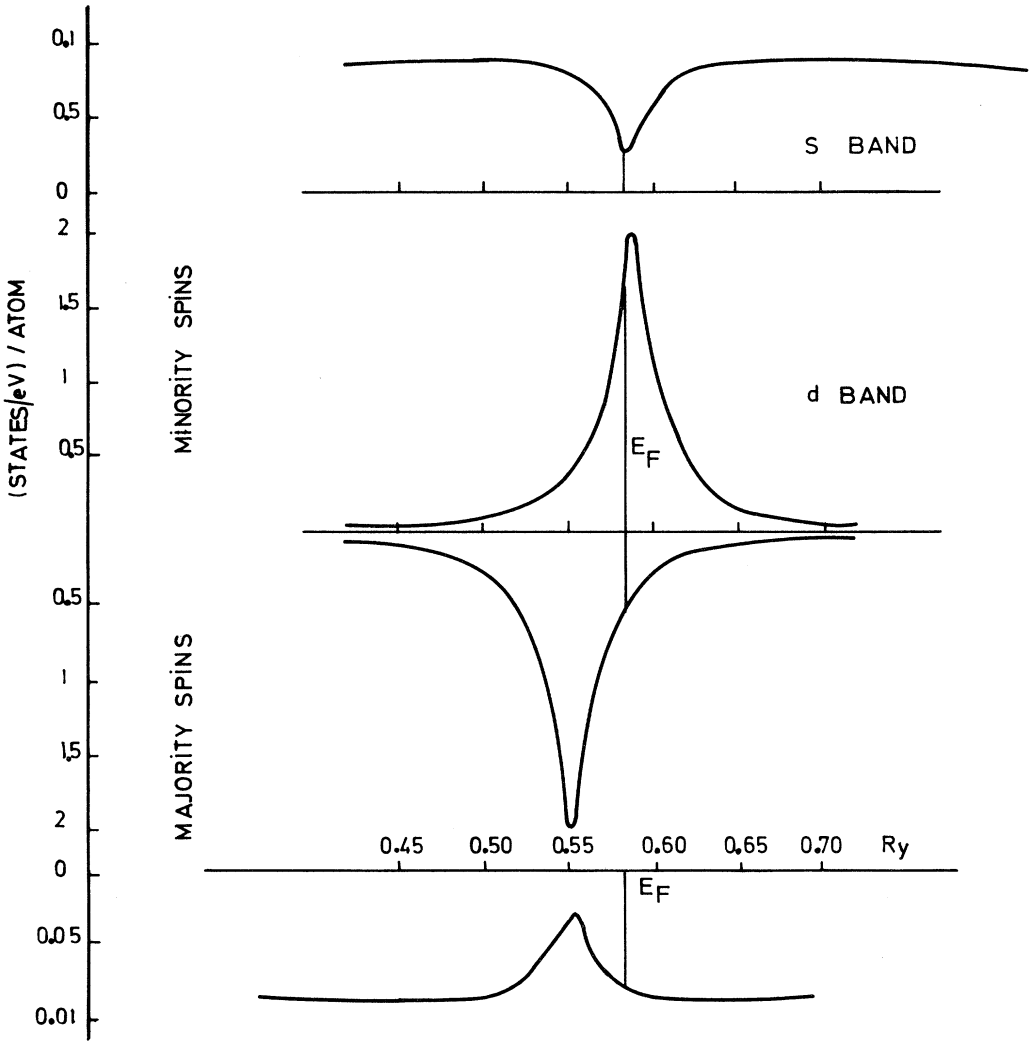

FIG. 3. s bands and the two upper peaks of the d bands used to represent ferromagnetic Ni.

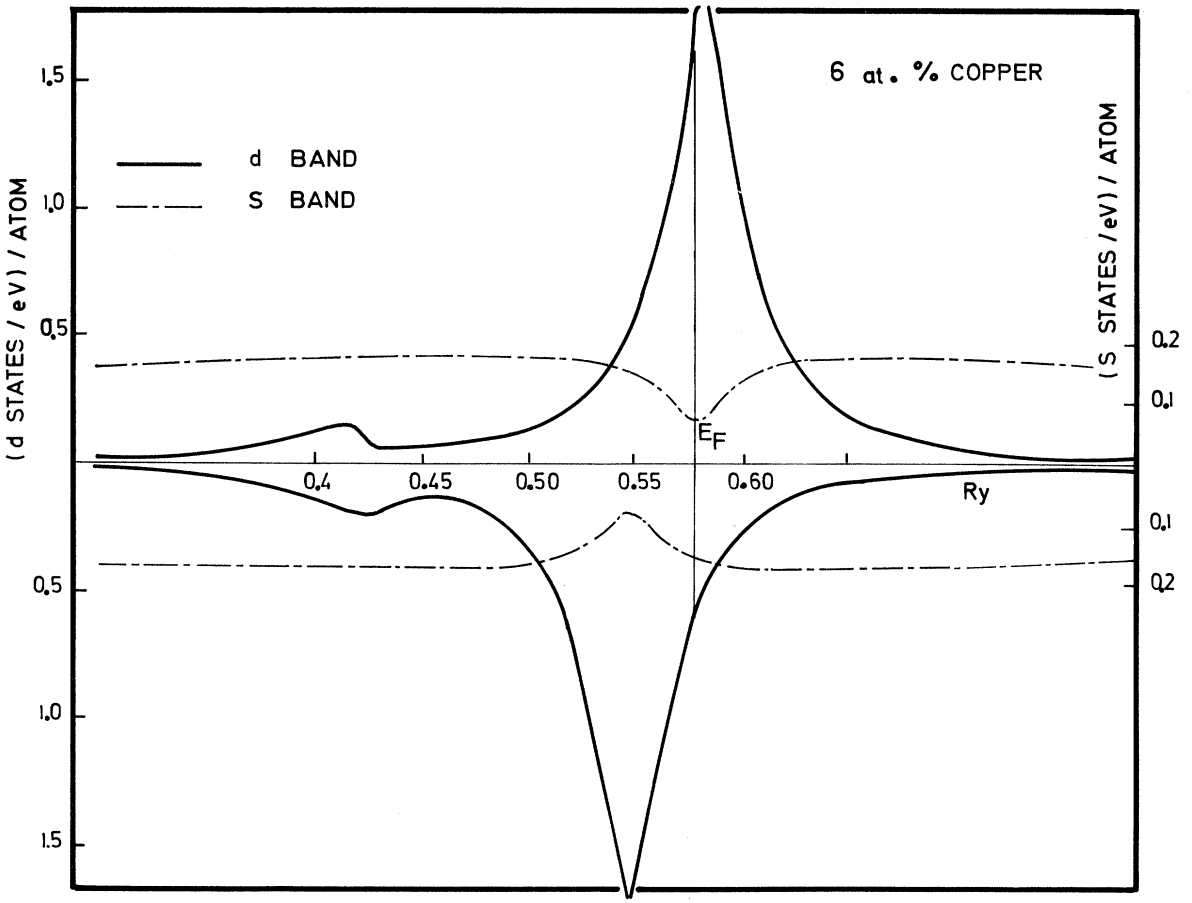

FIG. 4. s and d density of states of the artificial NiCu alloy for 6 at.% Cu.

tion on the s band: At first as the concentration of Cu increases $n_s(E_F)$ increases more rapidly than $n_d(E_F)$ decreases.

We now consider the electrical residual resistance ($T=0$ °K). Figure 8 exhibits the variation with concentration of the two resistivities $\rho\uparrow$ and $\rho\downarrow$. One can see that, up to about 6 at.% Cu in concentration, these two quantities vary linearly, and therefore in that range of concentration $\rho\downarrow/\rho\uparrow$ is constant. Figure 9 represents the ratio of resistivity down and up determined from Eq. (26) vs concentration. As we have seen, for small concentration of Cu (< 6 at.%) this ratio is constant and equal to 10, in agreement with the discussion of Campbell, Fert, and Jaoul.[10,11] For concentrations of Cu higher than 6 at.%, the quantity $\rho\downarrow/\rho\uparrow$ decreases steadily with concentration. The total resistivity calculated from Eq. (27) increases linearly with concentration (Fig. 10). This deviation from the usual $x(1-x)$ Nordheim's law agrees with experimental data. Figure 11 illustrates the final result of our paper. The calculated curve is in agreement with the few experimental data available, provided we take $\gamma_{so}=0.007$ in the dilute limit, a value which is very close to $\gamma_{so}\simeq 0.0075$ determined from various Ni-based alloys by Campbell, Fert, and Jaoul.[10,11] One can notice an increase of the anisotropy for concentrations smaller than 6 at.%. This feature is due to the decrease of the magnetization which gives rise to an increase of γ_{so} [Eq. (30)] in a region where $\rho\downarrow/\rho\uparrow$ is concentration independent. It would be interesting to investigate experimentally this small-concentration region for which no data are available in *Ni*Cu. By contrast in *Ni*Co one would obtain the opposite effect since the magnetization increases with the concentration of Co.

VII. CONCLUSIONS

In spite of its simplicity, the model described in this paper has been able to describe consistently in the framework of the CPA a number of independent experimental data. The variation with concentration of the majority- and minority-band density of states shows an almost linear decrease

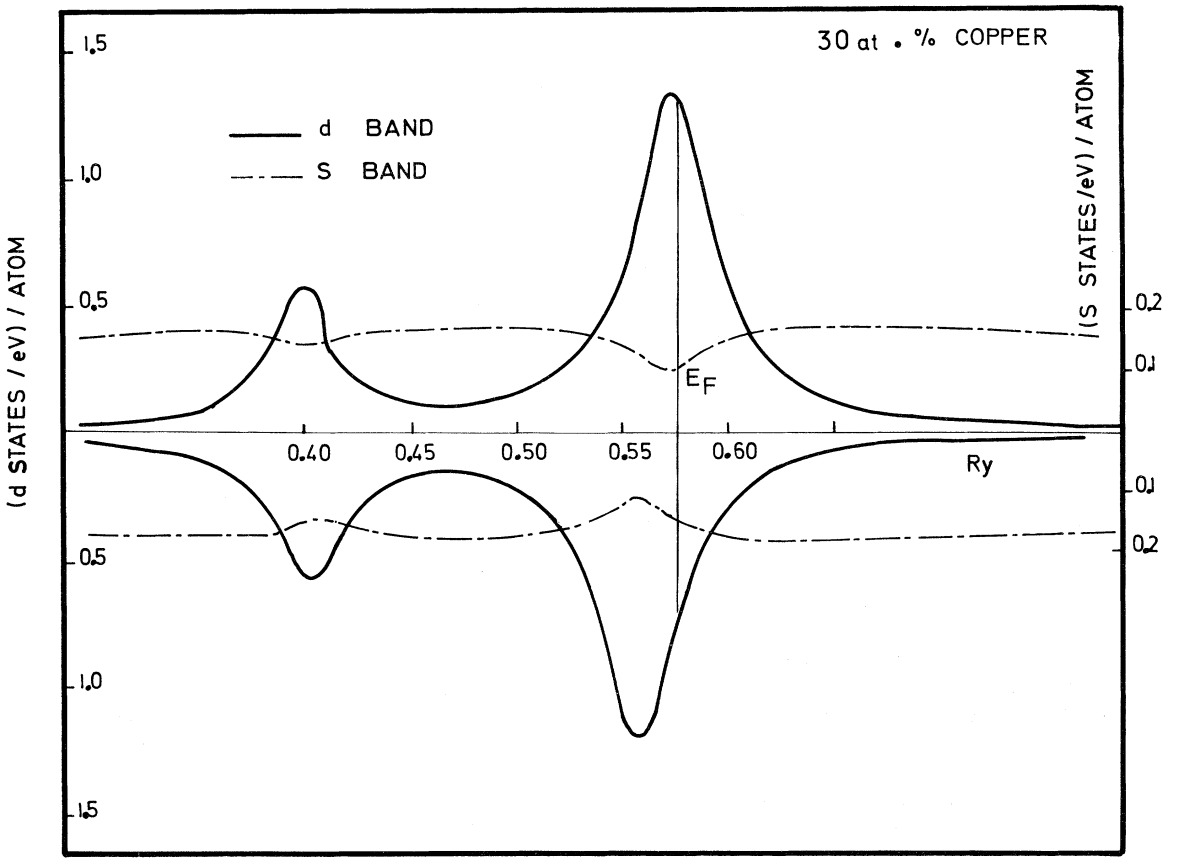

FIG. 5. s and d density of states of the artificial NiCu alloy for 30 at. % Cu.

of the magnetization as the concentration of Cu increases. As far as the residual conductivity is concerned, the most interesting result is the concentration dependence of the ratio $\rho\downarrow/\rho\uparrow$, which gives rise to a linear dependence of the total resistivity for concentrations smaller than 40 at. %

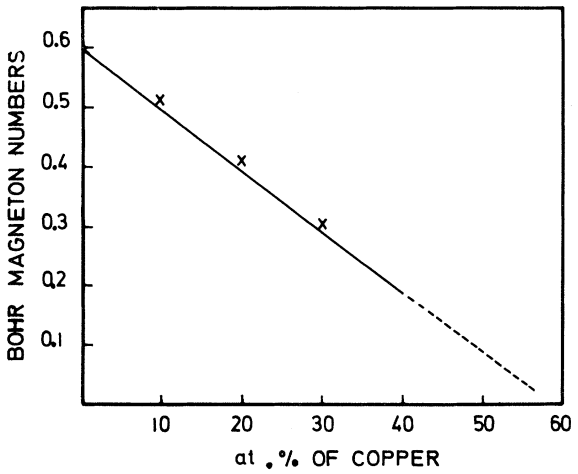

FIG. 6. Variation of magnetization with concentration for the NiCu model alloy. The crosses are experimental data. The numerical results are extrapolated beyond 40% (broken line).

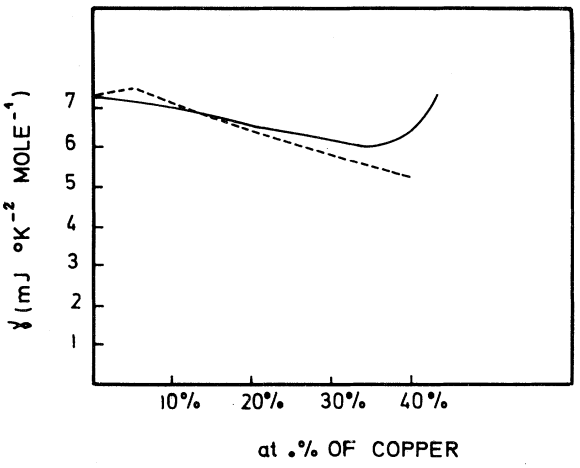

FIG. 7. Concentration dependence of the low-T specific-heat coefficient γ of NiCu (Ref. 23). The broken line represents the variation of the total density of states at the Fermi energy calculated in the present model.

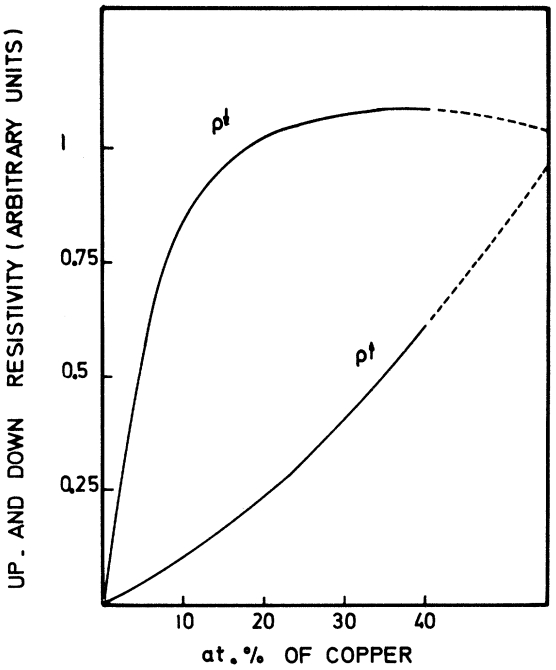

FIG. 8. Concentration dependence of the minority-band and majority-band resistivities $\rho_\downarrow$ and $\rho_\uparrow$.

Cu in Ni. In the dilute limit the ratio $\rho\downarrow/\rho\uparrow$ is 10. As a matter of fact, this order of magnitude can be guessed by considering the approximate expression obtained in Ref. 3 [Eq. (86)] for the relaxation time in the dilute limit when the d hopping is neglected. Here this relaxation time is spin dependent:

$$\tau_\sigma^{-1} = \left(\frac{\gamma_H}{\epsilon_F - \epsilon_{d,\sigma}^{\mathrm{Ni}}}\right)^2 (\epsilon_d^{\mathrm{Cu}} - \epsilon_{d,\sigma}^{\mathrm{Ni}})^2 n_{d,\sigma}^{\mathrm{Cu}}(E_F) \ . \qquad (32)$$

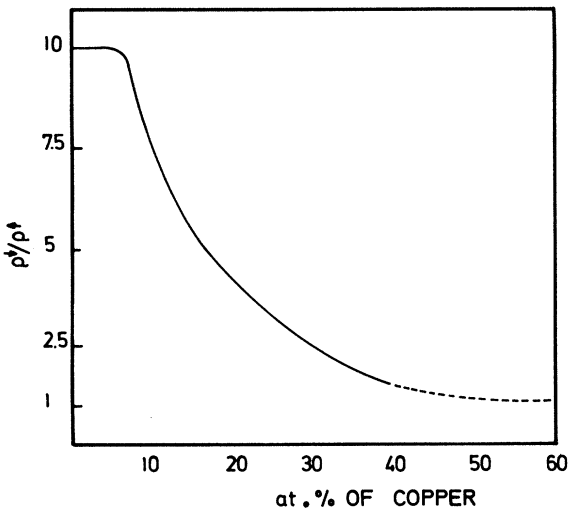

FIG. 9. Variation with concentration of the ratio minority-band to majority-band resistivities $\rho_\downarrow/\rho_\uparrow$.

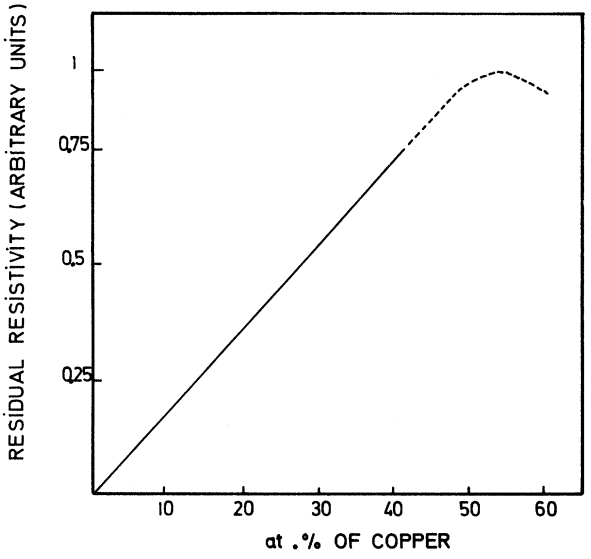

FIG. 10. Variation with concentration of the total residual resistivity.

For the minority band, the Fermi level is very close to $\epsilon_{d,\downarrow}^{\mathrm{Ni}}$ and the first factor is much larger in the minority band than in the majority band. This

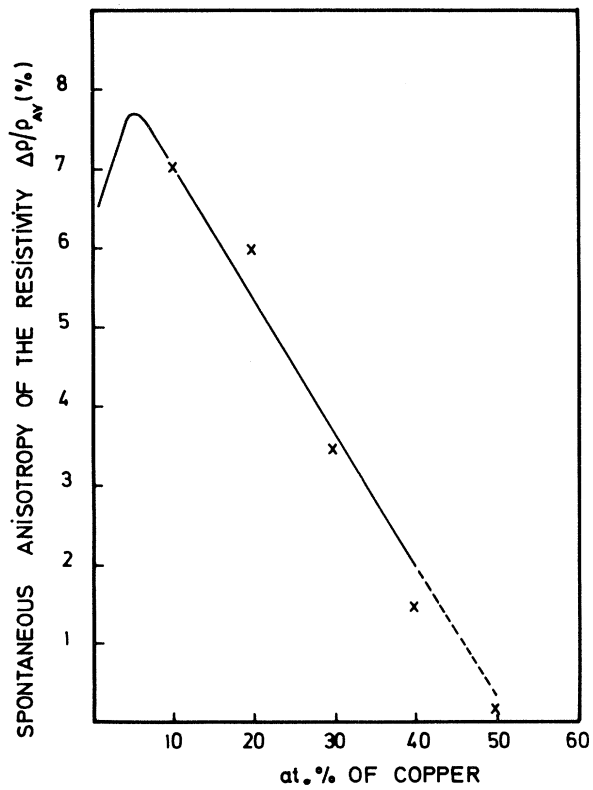

FIG. 11. Variation with concentration of the spontaneous anisotropy of the resistivity. The crosses correspond to experimental data compiled by Van Elst (Ref. 14).

difference underlines the effect of hybridization and its influence on the scattering in the minority band. Roughly, one has $(\epsilon_F - \epsilon_{d,\uparrow}^{Ni}) \simeq 4(\epsilon_F - \epsilon_{d,\downarrow}^{Ni})$. The second factor is slightly smaller in the minority band than in the majority band, while the third factor can be considered as independent of spin. If, moreover, we take account of the depletion of the s density of states at the Fermi energy in the minority band, one gets the calculated order of magnitude for $\rho\downarrow/\rho\uparrow$ in the dilute limit.

Because of the lack of experimental data, there is not a concensus[24] on the magnitude of $\rho\downarrow/\rho\uparrow$ in dilute *Ni*Cu. The value we get in our simplified model is in agreement with Smit's theory of the spontaneous anisotropy of resistance and is not in contradiction with the calculation of the resistance in pure Ni of Hasegawa *et al.*[25] These authors consider three Fermi surfaces in Ni. The first, a s Fermi surface, corresponds to the majority band, while the second and the third, s-d and d Fermi surfaces, correspond to the minority band where electrons at the Fermi level are strongly hybridized. The calculation of the resistivity due to phonon scattering in pure Ni indicates that in the ferromagnetic state the current is mainly carried by electrons on the s Fermi surface; in other words, the resistivity is much higher for minority-band electrons than for majority-band electrons. The results obtained in this paper for the disorder-induced resistivity lead to the same conclusion.

The extension of our calculations to a more realistic model for NiCu alloys and to other Ni-based alloys requires a development of the theory of the density of states and transport properties of ferromagnetic alloys. One should consider the details of the Fermi surface, the degeneracy of the d bands, and the k dependence of hybridization. This would involve the calculation of vertex corrections for the electrical conductivity. The difference of valence should be treated properly by considering charge transfer self-consistently, as is done in Ref. 4, and by investigating carefully the dilute concentration limit.

Finally, we want to emphasize the need for more experimental data in both dilute and nondilute concentration ranges.

ACKNOWLEDGMENTS

The first part of this paper was written while two of us (F. B. and A. V. V.) were working at Harvard University. They thank Professor Ehrenreich for his kind hospitality and encouragement. F. B. is very grateful to Professor Friedel for his interest in this work and for welcoming him in this laboratory. He also gratefully acknowledges helpful discussion with Dr. I. A. Campbell, Dr. F. Gautier, and Dr. A. Fert.

APPENDIX: AVERAGE t APPROXIMATION (ATA) IN FERROMAGNETIC ALLOYS

As demonstrated in Refs. 2 and 4, in the LEBV paramagnetic model, the non-self-consistent ATA is a good starting point for the self-consistent iteration calculation leading to the CPA. This is also the case in ferromagnetic alloys provided the ATA formulas of Refs. 2 and 4 are slightly modified to account for the dependence of $\epsilon_{d,\sigma}^{A(B)}$ on $N_{d,\sigma}^{A(B)}$.

In general, we choose the energy origin such that $\epsilon_{\text{para}}^{A} = -\epsilon_{\text{para}}^{B}$ and the ATA self-energy is given by[26]

$$\Sigma_d = \bar{\epsilon}_d^{\sigma} + \frac{\bar{t}_d^{\sigma}}{1 + F_{dd}^{\sigma}(z, \bar{\epsilon}_d^{\sigma})\bar{t}_d^{\sigma}} \quad , \tag{A1}$$

where $\bar{\epsilon}_d^{\sigma} = x\,\epsilon_{d,\sigma}^{A} + (1-x)\,\epsilon_{d,\sigma}^{B}$ [Eq. (15)] and $\epsilon_{d,\sigma}^{A(B)} = \epsilon_{\text{para}}^{A(B)} - U_{\text{eff}}^{A(B)}(N_{d,-\sigma}^{A(B)} - N_{d,-\sigma}^{A(B)\text{para}})$ [Eq. (12)], and

$$\bar{t}_d^{\sigma} = x\,\frac{\epsilon_{d,\sigma}^{A} - \bar{\epsilon}_d^{\sigma}}{1 - (\epsilon_{d,\sigma}^{A} - \bar{\epsilon}_d^{\sigma})F_{dd}^{\sigma}(z, \bar{\epsilon}_d^{\sigma})} + (1-x)\,\frac{\epsilon_{d,\sigma}^{B} - \bar{\epsilon}_d^{\sigma}}{1 + (\epsilon_{d,\sigma}^{B} - \bar{\epsilon}_d^{\sigma})F_{dd}^{\sigma}(z, \bar{\epsilon}_d^{\sigma})} \quad . \tag{A2}$$

If we substitute (A2) into (A1), we get finally

$$\Sigma_d^{\sigma} = \bar{\epsilon}_d^{\sigma} - \frac{(\epsilon_{d,\sigma}^{A} - \bar{\epsilon}_d^{\sigma})(\epsilon_{d,\sigma}^{B} - \bar{\epsilon}_d^{\sigma})F_{dd}^{\sigma}(z, \bar{\epsilon}_d^{\sigma})}{1 + (2\bar{\epsilon}_d^{\sigma} - \epsilon_{d,\sigma}^{A} - \epsilon_{d,\sigma}^{B})F_{dd}^{\sigma}(z, \bar{\epsilon}_d^{\sigma})} , \tag{A3}$$

which is the ATA expression for the self-energy in the ferromagnetic LEBV model.

---

*Preliminary results were presented at the Conference on Band Structure Spectroscopy of Metals and Alloys, Strathclyde University, Glasgow, Scotland, 1971.

†Permanent address: Institut de Physique, Université de Liège, Sart-Tilman, Liège, Belgium.

‡Laboratoire associé au Centre National de la Recherche Scientifique.

[1] K. Levin and H. Ehrenreich, Phys. Rev. B 3, 4172 (1971).

[2] L. Schwartz, F. Brouers, A. V. Vedyayev, and H. Ehrenreich, Phys. Rev. B 4, 3383 (1971). F. Brouers, H. Ehrenreich, L. Schwartz, and A. V. Vedyayev, in Proceedings of the Conference on Perspective for Computation of Electronic Structures in Ordered and Disordered Solids, Menton, 1971 (unpublished).

[3] F. Brouers and A. V. Vedyayev, Phys. Rev. B 5, 348 (1972).

[4] F. Brouers and A. V. Vedyayev, in *Band Structure Spectroscopy of Metal and Alloys*, edited by D. Fabian (Academic, New York, 1972).

[5] J. Kudrnovsky, Ph. D. thesis (Prague University, 1971) (unpublished); B. Velicky (private communication).

[6] P. Soven, Phys. Rev. 156, 809 (1967).

[7] P. Soven, Phys. Rev. 178, 1138 (1969).

[8] B. Velicky, S. Kirkpatrick, and H. Ehrenreich, Phys. Rev. 175, 747 (1968).

[9]J. Smit, Physica 16, 612 (1951).
[10]I. A. Campbell, Phys. Rev. Letters 24, 269 (1970).
[11]I. A. Campbell, A. Fert, and O. Jaoul, J. Phys. C Suppl. 1, S95 (1970).
[12]N. F. Mott, Proc. Roy. Soc. (London) A153, 699 (1936).
[13]B. Velicky, Phys. Rev. 184, 614 (1969).
[14]H. C. Van Elst, Physica 25, 708 (1959).
[15]H. Hasegawa and J. Kanamori, J. Phys. Soc. Japan 31, 382 (1971).
[16]It is worth noticing that Smit's theory assumes that the majority band is completely filled. In our model, because of hybridization, there are a few holes in that band. To be rigorous, Smit's theory should be extended and we would write $\rho_{\uparrow}^{\parallel}=\rho_{\uparrow}^{\perp}+\gamma_{so}\rho_{\downarrow}-\gamma'_{so}\rho_{\uparrow}$. The third term is, however, much smaller than the second and as a first approximation we can neglect this contribution in Eq. (28).
[17]L. Hodges, H. Ehrenreich, and N. D. Lang, Phys. Rev. 152, 505 (1966).
[18]V. Heine, Phys. Rev. 153, 673 (1967).
[19]E. P. Wohlfrath, J. Appl. Phys. 41, 1205 (1970).
[20]If we want to compare U_{eff} with other estimations, we have to consider its value for one orbital: 0.9 eV $\times 1.5$, a value between 1.25 (Herring) and 2.65 [Hodges *et al.* (Ref. 17)].
[21]P. M. Tedrow and R. Meservey, Phys. Rev. Letters 26, 192 (1971).
[22]V. Bänninger, G. Busch, M. Campagna, and H. C. Siegmann, Phys. Rev. Letters 25, 585 (1970).
[23]M. Dixon, F. E. Hoare, and T. M. Holden, Proc. Roy. Soc. (London) A303, 339 (1968).
[24]F. Gautier (private communication).
[25]A. Hasegawa, S. Wakoh, and J. Yamashita, J. Phys. Soc. Japan 20, 1865 (1965).
[26]Cf. Eq. (25) of Ref. 4, with $\sigma_d=\bar{\epsilon}_d$.

PHYSICAL REVIEW B VOLUME 7, NUMBER 1 1 JANUARY 1973

Excitation Spectrum of Magnetic Domain Walls

A. A. Thiele
Bell Laboratories, Murray Hill, New Jersey 07974
(Received 18 May 1972)

The eigenvalue equation for the normal modes of excitation of a moving infinite planar magnetic domain wall in an infinite material having the most general second-rank tensor anisotropy is presented. The eigenvalues and eigenfunctions of both the spin waves in the presence of the moving wall and the excitation of the wall itself are given to first order in velocity. Cylindrical-domain resonance experiments are proposed to test for the existence of the excitation modes and their effect on domain propagation. The dispersion relation for the wall excitation modes is found to imply a new material requirement for high mobility.

I. INTRODUCTION

The excitation spectrum of an infinite planar 180° domain wall in an infinite magnetic material having a constant magnetization magnitude M_s is treated here in the continuum approximation. For the description of this system, Cartesian tensors in a right-handed coordinate system and Euler angles will be used. The position in the material is denoted by x_j, and only the polar (θ) and azimuthal (φ) Euler angles are used. The polar axis is the x_3 direction, and φ is zero in the x_1 direction. Vectors as well as their components will be denoted by symbols of the form v_j and, similarly, tensors will be denoted by symbols of the form T_{jk}. Repeated indices are understood to be summed from 1 to 3. The totally antisymmetric unit tensor is denoted by e_{kjp}.

II. MAGNETIC ENERGY DENSITY

The material is taken to have the most general second-rank tensor anisotropy. When the coordinate system is properly oriented with respect to the crystalline axes and when the arbitrary zero of energy is chosen so that the lowest value of the anisotropy energy is zero, the anisotropy energy density may be written

$$\rho_K=(1/M_s^2)K_{jk}M_jM_k\,, \tag{1a}$$

where M_j is the magnetization vector and

$$K_{jk}\equiv\begin{bmatrix}K_u & 0 & 0\\ 0 & K_u+K_o & 0\\ 0 & 0 & 0\end{bmatrix}\,,\quad K_u>0\,,\quad K_o>0 \tag{1b}$$

(u for uniaxial and o for orthorhombic). The anisotropy energy is minimized when $M_j=[0,0,\pm M_s]$. In a bubble domain device, such a material would be oriented with the plate normal along the polar (3) axis and the domain-wall normals in the 1,2 plane. Attention will subsequently be restricted to a planar domain wall whose wall normal lies in the 1, 2 plane, for which the local demagnetizing energy density between two regions having $M_3=\pm M_s$ is

$$\rho_d=2\pi(n_jM_j)^2 \tag{2a}$$

$$=2\pi n_jn_kM_jM_k\,. \tag{2b}$$